IBRO Neuroscience Reports 16 (2024) 135–146

Contents lists available at ScienceDirect

IBRO Neuroscience Reports

journal homepage: www.sciencedirect.com/journal/IBRO-Neuroscience-Reports

Research paper

Assessing remission in major depressive disorder using a functional-structural data fusion pipeline: A CAN-BIND-1 study

Sondos Ayyash [a,b], Andrew D. Davis [c,d], Gésine L. Alders [e], Glenda MacQueen [f,g], Stephen C. Strother [d,h,i], Stefanie Hassel [f,g], Mojdeh Zamyadi [d], Stephen R. Arnott [d], Jacqueline K. Harris [j], Raymond W. Lam [k], Roumen Milev [l], Daniel J. Müller [m,n], Sidney H. Kennedy [h,n,o,p,q], Susan Rotzinger [n,p,q], Benicio N. Frey [c,e,r], Luciano Minuzzi [c,e,r], Geoffrey B. Hall [a,b,c,e,*], CAN-BIND Investigator Team

[a] School of Biomedical Engineering, McMaster University, Hamilton, Ontario, Canada
[b] Department of Psychology, Neuroscience & Behaviour, McMaster University, Hamilton, Ontario, Canada
[c] Department of Psychiatry and Behavioural Neurosciences, McMaster University, Hamilton, Ontario, Canada
[d] Rotman Research Institute, Baycrest, Toronto, Ontario, Canada
[e] Neuroscience Graduate Program, McMaster University, Hamilton, Ontario, Canada
[f] Hotchkiss Brain Institute and Mathison Centre for Mental Health Research and Education, Cumming School of Medicine, University of Calgary, Calgary, Alberta, Canada
[g] Department of Psychiatry, Cumming School of Medicine, University of Calgary, Calgary, Alberta, Canada
[h] Institute of Medical Science, University of Toronto, Toronto, Ontario, Canada
[i] Department of Medical Biophysics, University of Toronto, Ontario, Canada
[j] Department of Computer Science, University of Alberta, Edmonton, Alberta, Canada
[k] Department of Psychiatry, University of British Columbia, Vancouver, British Columbia, Canada
[l] Departments of Psychiatry and Psychology, Queen's University, Providence Care Hospital, Kingston, Ontario, Canada
[m] Campbell Family Mental Health Research Institute, Centre for Addiction and Mental Health, Toronto, Ontario, Canada
[n] Department of Psychiatry, University of Toronto, Toronto, Ontario, Canada
[o] Centre for Mental Health, University Health Network, Toronto, Ontario, Canada
[p] Krembil Research Institute, University Health Network, Toronto, Ontario, Canada
[q] Centre for Depression and Suicide Studies, and Li Ka Shing Knowledge Institute, St. Michael's Hospital, Toronto, Ontario, Canada
[r] Mood Disorders Treatment and Research Centre and Women's Health Concerns Clinic, St. Joseph's Healthcare, Hamilton, Ontario, Canada

ARTICLE INFO

Keywords:
Neuroimaging
Major depressive disorder
Structural connectivity
Functional connectivity
Data fusion
Resting brain networks
Toolbox

ABSTRACT

Neural network-level changes underlying symptom remission in major depressive disorder (MDD) are often studied from a single perspective. Multimodal approaches to assess neuropsychiatric disorders are evolving, as they offer richer information about brain networks. A *FATCAT-awFC* pipeline was developed to integrate a computationally intense data fusion method with a toolbox, to produce a faster and more intuitive pipeline for combining functional connectivity with structural connectivity (denoted as anatomically weighted functional connectivity (*awFC*)). Ninety-three participants from the Canadian Biomarker Integration Network for Depression study (CAN-BIND-1) were included. Patients with MDD were treated with 8 weeks of escitalopram and adjunctive aripiprazole for another 8 weeks. Between-group connectivity (SC, FC, *awFC*) comparisons contrasted remitters (REM) with non-remitters (NREM) at baseline and 8 weeks. Additionally, a longitudinal study analysis was performed to compare connectivity changes across time for REM, from baseline to week-8. Association between cognitive variables and connectivity were also assessed. REM were distinguished from NREM by lower *awFC* within the default mode, frontoparietal, and ventral attention networks. Compared to REM at baseline, REM at week-8 revealed increased *awFC* within the dorsal attention network and decreased awFC within the frontoparietal network. A medium effect size was observed for most results. *AwFC* in the frontoparietal network was associated with neurocognitive index and cognitive flexibility for the NREM group at week-8. In conclusion, the *FATCAT-awFC* pipeline has the benefit of providing insight on the 'full picture' of connectivity changes for REMs and NREMs while making for an easy intuitive approach.

* Corresponding author at: Department of Psychology, Neuroscience & Behaviour, McMaster University, Hamilton, Ontario, Canada.

https://doi.org/10.1016/j.ibneur.2023.12.011
Received 24 September 2023; Accepted 30 December 2023
Available online 4 January 2024

1. Introduction

Major depressive disorder (MDD) is one of the most common mental health disorders affecting approximately 163 million people worldwide, accounting for high levels of morbidity, mortality and psychosocial functional impairment (James et al., 2018). Antidepressants are one of a number of treatment options used in the management of MDD (Gautam et al., 2017; Kennedy et al., 2016). Selective serotonin reuptake inhibitors (SSRIs) are often the first choice of antidepressant treatment for MDD (Cipriani et al., 2016; Middleton et al., 2005). One of the most commonly prescribed SSRIs for the treatment of MDD is escitalopram (Kaplan and Zhang, 2012).

Clinical remission has become the gold standard and primary goal of MDD treatment (Ballenger, 1999; Khoo et al., 2015; McIntyre et al., 2006; Stahl, 1999). The Diagnostic and Statistical Manual-IV (DSM-IV-TR) (Diagnostic and statistical manual of mental disorders (2000)) defines remission in MDD as the 'absence or near absence of the signs and symptoms' of depression. Other important characteristics of MDD remission after treatment include: the feeling of a return to their normal self, improved mental health, and improved functioning (Zimmerman et al., 2006). As such it is of interest to study the effect behavioural changes have on brain connectivity in MDD remission. It is in the MDD remitters that we expect to see changes in connectivity after treatment, because it has been extensively documented that MDD remitters show improved behavioural performance (Zimmerman et al., 2006). However, although symptom remission has become the primary goal of MDD treatment, remission rates vary from 30 to 50% in research-based, 6–14-week trials, involving symptomatic participants with MDD (Thase et al., 2005, 2010; Trivedi et al., 2006). In addition, participants with MDD who fail to attain remission status from one round of antidepressant treatment, have a much lower remission rate with each subsequent treatment attempt (Rush et al., 2006). Non-remission in MDD is often associated with higher healthcare resource utilization and costs (Byford et al., 2011; Dennehy et al., 2015; Kubitz et al., 2013; Mauskopf et al., 2009).

Previous neuroimaging studies in MDD have used structural connectivity (SC) and functional connectivity (FC) to identify neural biomarkers for the prediction of treatment outcomes, including remission (Korgaonkar et al., 2014, 2020). Building on this work, examining the brain connectivity changes in patients with remitted MDD (REM) and patients with non-remitted MDD (NREM) may provide us with a better understanding of the underlying, network-level differences that distinguish these two groups. Alongside clinical remission, cognitive remission is a goal in the treatment of MDD (McIntyre et al., 2013). Cognitive dysfunction is one of the most common symptoms of MDD (Fava et al., 2006; Lee et al., 2012). Cognitive dysfunction impacts multiple cognitive domains such as memory, difficulty in decision making, and loss of cognitive flexibility (Jaeger et al., 2006; McCall and Dunn, 2003; Naismith et al., 2007). While general symptom remission may be achieved with pharmacotherapy, cognitive dysfunction may persist (Conradi et al., 2011; Hasselbalch et al., 2011; Snyder, 2013). Many of the same brain regions that play a role in these cognitive dysfunctions are implicated in MDD (Albert et al., 2019). Therefore, because of this overlap we want to try and understand the association between those cognitive domains and remission. Reports of cognitive deficits in REM have been inconsistent, with some reports of cognitive improvements (Abo Aoun et al., 2019; Gudayol-Ferré et al., 2015) and other studies reporting persistent cognitive deficits (Bhalla et al., 2006; Conradi et al., 2011; Reppermund et al., 2009).

Combining SC and FC data can capture unique and complimentary aspects of the underlying Resting State Networks (RSN) in REM and NREM. This study focuses on connectivity within five RSNs affected in MDD: the default mode network (DMN), dorsal attention network (DAN), ventral attention network (VAN), frontoparietal network (FPN), and limbic network (LIM). These five networks were drawn from the 7-network model suggested by Buckner et al. (2011). The visual and auditory networks were excluded, similar to a meta-analysis of FC conducted by Kaiser et al. (2015a), which specifically investigated RSNs implicated in MDD.

Both structural and functional network-level connectivity changes within RSNs have shown connectivity changes associated with remission status (REM or NREM after treatment), both at baseline and after a course (e.g. 8 weeks) of antidepressant treatment. Karim et al. (2017) assessed resting-state FC at different intervals starting at baseline and ending at week-12. They found that REM showed decreased connectivity in the DMN from baseline to week-12, whereas there was increased connectivity in the executive control network, part of the DAN. These findings were attributed to a reduction in rumination and anxiety and greater cognitive control (Karim et al., 2017). These patterns appear to fit within the framework that MDD is characterized by functional under-activity particularly in the executive control network (i.e. pre- and post-central gyrus), and with response to antidepressant treatment there is a shift toward normalized function that is reflected in either strengthening or weakening of brain connections within the executive control network or the DMN (Karim et al., 2017). Studies have also assessed whether FC and SC after antidepressant treatment can distinguish remission status (REM vs NREM). A study by Xiao et al. (2019), found that rapid remission (within 1–5 days) was associated with lower FC between several brain regions (i.e. between subgenual cingulate cortex and DMN nodes) (Xiao et al., 2019). Additionally, Pillai et al. (2019) performed an SC analysis using fractional anisotropy (FA) after 8 weeks of antidepressant treatment and reported lower SC between the raphe nucleus and amygdala for REM compared to NREM. Hence, treatment of MDD is associated with either increases or decreases of connectivity, reflecting normalization – also known as reversal – of the connectivity patterns observed with MDD prior to medication therapy (Wang, Xia, et al., 2014). Combining SC and FC may then provide a more comprehensive understanding of brain changes and their association with clinical variables in REM and NREM (Zheng et al., 2018). Treatment of MDD is accompanied with either increases or decreases of connectivity, reflecting normalization – also known as reversal - of the connectivity patterns observed with MDD prior to medication therapy (Wang et al., 2014).

For this project, we examined neuroimaging and clinical data from the Canadian Biomarker Integration Network for Depression study (CAN-BIND-1) comprised of patients with MDD treated with escitalopram alone and with adjunctive aripiprazole (Kennedy et al., 2019; Lam et al., 2016). The goal was to evaluate whether network-level differences can be detected (1) between REM and NREM groups at baseline, (2) between REM and NREM groups at week-8, and (3) within the REM group between baseline and week-8. We applied a *FATCAT-awFC* pipeline, developed in our previous work (Ayyash et al., 2021), that involves the combination of the *Functional and Tractographic Connectivity Analysis Toolbox* (*FATCAT*) (Taylor and Saad, 2013) with a computationally intense method, known as the *Anatomically-Weighted Functional Connectivity* (*awFC*) *method* (Bowman et al., 2012). Our previous work (Ayyash et al., 2021), identified that combining metrics from different modalities in a multiplicative manner, provides robust findings whereby the cost associated with the weaker modality is reduced and significant patterns are highlighted. In addition, to study traditional FC and SC within RSNs, we also performed separate and comparative brain connectivity analyses between FC, SC, and *awFC*. Finally, we explored the association of brain connectivity changes with cognition in RSNs within the REM and NREM groups at baseline and week-8. We hypothesized that NREM will produce lower connectivity strength between brain regions compared to REM, at baseline and week-8. This hypothesis is based on the study by Korgaonkar et al. (2020), who demonstrated that at pre-treatment (baseline) NREM displayed lower functional connectivity compared to REM, which was amplified post-treatment (week 8). Krause-Sorio et al. (2020) also demonstrated that higher structural connectivity (measured as fractional anisotropy) was associated with greater improvement in depressive symptoms. Thus, according to the

literature, reduced connectivity for both structure and function were indicative of improved depressive symptoms (remission). We also hypothesized that the REM group will have reduced connectivity from baseline to week-8, as it has been previously shown that a decrease in DMN and Salience network were indicative of reduced rumination and anxiety (Karim et al., 2017). Finally, we hypothesized that connectivity strength will be associated with cognitive changes in the REM and NREM groups at week-8.

2. Materials and methods

2.1. Participants in CAN-BIND-1

2.1.1. Inclusion and exclusion criteria

The included 211 participants from six Canadian academic health science institutions (Kennedy et al., 2019; Lam et al., 2016; MacQueen et al., 2019). For more detailed information of imaging and clinical protocols, refer to (Lam et al., 2016; MacQueen et al., 2019). At each institution, the research protocol was reviewed and approved by the respective research ethics board. The inclusion criteria for these participants included: 18–60 years of age; diagnosis of MDD by DSM-IV-TR criteria and confirmed with the Mini International Neuropsychiatric Interview (Sheehan et al., 1998); and a Montgomery-Åsberg Depression Rating Scale (MADRS) (Montgomery and Asberg, 1979) score $\geq$ 24. If previously taking antidepressants, a medication washout of at least five half-lives was required. The exclusion criteria included: diagnosis of psychosis, bipolar I/II disorder, substance use disorder (in the past 6 months), prior brain injury, and prior neurological diseases; four failed trials of pharmacological intervention; history of non-response or intolerance to escitalopram, pregnant or breastfeeding, high suicidality risk; and any magnetic resonance imaging contraindications (MacQueen et al., 2019). Written, informed consent was obtained from all participants before participation in the study, and participants received compensation for their time and effort.

2.1.2. Treatment

Following baseline testing, MDD patients began treatment with the SSRI escitalopram, at an initial dose of 10 mg/d, which was then increased (up to 20 mg/d) at week-2 or week-4 if a 20% or 50% MADRS reduction from baseline was not observed, respectively (Lam et al., 2016). All participants took escitalopram in the first phase of the study (duration of 8 weeks). In phase 2, responders (defined as MADRS reduction from baseline to Week 8 $\geq$50%) continued to take escitalopram alone, while non-responders were given adjunctive aripiprazole (0.5–2 mg/d) for another 8 weeks. Data were collected at baseline before medication treatment and at week-8 after 8 weeks of escitalopram treatment.

2.1.3. Cognitive testing

The CNS-Vital Signs (CNS-VS) a computerized cognitive test battery was used to assess participants' level of cognitive functioning (Gualtieri and Johnson, 2006). Five cognitive subscales of the CNS-VS test were examined: memory, cognitive flexibility, complex attention, processing speed and neurocognitive index (a summary score that collectively examines the five cognitive variables: complex attention, memory, psychomotor speed, reaction time, and cognitive flexibility) (Iverson et al., 2009).

2.2. fMRI data acquisition and processing

The rsfMRI scanning was performed on 3.0 T scanners (Three Discovery MR750 from GE Healthcare, USA; One Intera from Phillips, Netherlands; One Signa HDxt from GE Healthcare, USA; One Trio Tim from Siemens, Germany). For rsFMRI acquisition the participants were asked to lay still in the MRI scanner with eyes open, looking at a fixation cross for 10 min. Functional images were acquired with an echo planar imaging (EPI) sequence with the following parameters: repetition time (TR)/echo time (TE) = 2000/30 ms, 36–40 axial slices, 64 × 64 matrix, 75° flip angle, 256 mm field of view (FOV) (exception: Queens site FOV =1536 mm), 4 mm section thickness, with no slice gap, and 300 volumes with one run per session.

2.3. T1-Weighted image acquisition

Anatomical reference scans were obtained with the following parameters: TR/TE/flip angle: 6.4–7.5 ms/2.7–3.5 ms/8–15° (exception: Siemens Scanners TR = 1760, 1840 ms), inversion time: 450–950 ms, voxel size: 1 × 1 × 1 mm^3, matrix dimensions 240 × 240 and 256 × 256, slice thickness: 1 mm, number of slices: 155–192. Time of acquisition for anatomical scans varied from 3:30 to 9:53 min. For more information, see (Lam et al., 2016; MacQueen et al., 2019).

2.4. fMRI preprocessing

The software package, Optimization of Preprocessing Pipelines for NeuroImaging-fMRI (OPPNI) was employed for image preprocessing (Churchill et al., 2015; Strother, 2006). For fMRI images, the first five images were discarded to control for destabilization of the magnetic field at scan start. To correct for participant movement during the scan a principal component analysis (PCA) was used to calculate the Euclidean distance of each volume from the median coordinates. The volume with the smallest Euclidean distance from the mean was selected to be the reference volume, and was then utilized in the motion correction step, applying AFNI's *3dvolreg* function. To mitigate the effects of participant motion, rigid-body realignment was performed, whereby subsequent time-series volumes were transformed to match the reference volume. In the censoring step, slices that were identified as outliers were replaced by interpolated values from neighboring time points via cubic splines. Fourier interpolation was used to correct for timing offsets between interleaved axial slices using AFNI's *3dTshift* (*TIMECOR*), a slice-timing correction function. fMRI images were then smoothed using the *3dBlurToFWHM* command in AFNI at full width half maximum = 6 mm in the x y z directions. Participant-specific non-neuronal tissue masks were generated via the *PHYCAA+* algorithm and a second-order Legendre polynomial was used for temporal detrending. The Legendre polynomial is a temporal detrending model that is used to remove low frequency trends and artefacts (Ombao et al., 2016). The six motion parameters obtained from the motion correction step were regressed out using PCA. Principal components explained 85% of the variance of the motion parameters. In addition, nuisance regressors (such as cerebrospinal fluid, white matter, and global signal) were used as temporal covariates and regressed out. Participants with a high mean framewise displacement (>0.2 mm) (Jenkinson et al., 2002) or long spike volumes that resulted in less than 5 min of signal, were excluded. Finally, a low-pass filter was applied to the functional data to remove physiological noise with a frequency cut-off of 0.1 Hz.

2.5. Resting-state functional connectivity analysis

The *FATCAT-awFC* pipeline has two inputs; one is from functional data (rsfMRI) and the second is from structural data (DTI). First, the functional data is fed into the *FATCAT* pipeline. Our previous work (Ayyash et al.,2021) details the application of the *FATCAT* pipeline (Taylor and Saad, 2013) in anatomically weighted-functional connectivity analyses. To begin, resting-state functional data was evaluated using group independent component analysis (gICA) applying temporal concatenation with FSL's Multivariate Exploratory Linear Decomposition into Independent Components (*MELODIC*) version 6.0 (Griffanti, 2019). Data from REM and NREM participants were combined in the gICA analysis. The group ICA identifies the main overlapping brain regions from concatenated individual data; the dimensionality was selected to be 20 components. A dimensionality of 20 was chosen as it

consistently produces similar large-scale resting state fMRI networks (Ray et al., 2013; Smith et al., 2009), as demonstrated across many studies (e.g. Brennan et al., 2022; Chaddock-Heyman et al., 2018; Cochereau et al., 2016). Each gICA component was compared to the Yeo 7-network map to identify RSNs (Yeo et al., 2011). Dice coefficients were calculated using *FATCAT's 3dMatch* tool (Taylor & Saad, 2013) and subsequently the highest dice coefficient was used to identify the independent component (IC) that most closely resembled the Yeo et al. (2011) template (Yeo et al., 2011). This was further validated by visual inspection. *FATCAT's 3dROIMaker* (Taylor and Saad, 2013) step was applied to threshold the spatial maps (DMN, Z = 3.4; FPN, Z = 5.4; DAN, Z = 0.85; VAN, Z = 3; LIM, Z = 1.3). Network parcellation thresholds were selected for the spatial maps with a visual similarity to networks observed in the Yeo network and were similar to the standard networks in the literature (Kaiser et al., 2015b; Yeo et al., 2011). These networks ranged in complexity from 3–5 nodes. The group-derived regions of interest (ROIs) were then projected on to each participant's functional data and *FATCAT's 3dNetCorr* (Taylor and Saad, 2013) tool was used to calculate correlations between the mean time-series of region pairs within each network for each participant. A set of inflated ROIs (increased outer boundary by two voxels) was also produced using *3dROIMaker* for use in the diffusion side of the pipeline that followed.

2.6. DTI Data acquisition and processing

Diffusion weighted imaging was conducted using a single-shot spin-echo EPI sequence. Diffusion gradients at b = 1000 s/mm^2, were applied sequentially along 31 non-collinear directions in most sites (exceptions, Queens: 30, University of British Columbia: 30). An additional scan without diffusion sensitizing at B= 0 s/mm^2 was also collected. The DTI acquisition protocol included one-signal averages of a whole brain sequence: TR = 8000 ms (exception: University of British Columbia: 9000), TE = 94 ms, FOV: 240 × 240 mm, matrix: 96 × 96 with 52–58 slices, voxel size: 2.5 mm^3, acceleration factor R = 2, with an acquisition duration of approximately 5 min for one dataset. Image space reconstruction (i.e. GE ASSET, Phillips SENSE) was used for most sites, except for 3 sites that used the GRAPPA k-space method.

2.7. DTI preprocessing

Each DTI volume was co-registered using affine transformation (FSL *eddy_correct* tool) to the first B_0 volume to correct for motion and eddy current. B-values were rotated accordingly. Data were then skull stripped, and a diffusion tensor reconstruction was calculated using a weighted least squares fit and FA maps were created. All the participant's FA data were then aligned onto a standard 2-mm FMRIB58 FA template (Webster, 2012) using the non-linear registration tool *FNIRT*. FSL's tract-based spatial statistics was used to project each participant's FA maps onto the skeletonized mean-FA template (to avoid partial volume effects).

2.8. DTI analysis

The *FATCAT-awFC* pipeline requires data from two sources; the functional RS data and the structural diffusion data. The diffusion data was processed using the FATCAT pipeline (Taylor and Saad, 2013) as shown in Ayyash et al. (2021). Bayesian estimation of diffusion parameters were determined using FSL's Bayesian Estimation of Diffusion Parameters Obtained using Sampling Techniques (*BEDPOSTX*). Uncertainty estimates for DTI parameters (FA and first eigenvector) were determined for each participant, using FATCAT's *3dDWUncert* (Taylor and Saad, 2013) with 300 iterations (Jackknife resampling). DTI parameters and uncertainty measures were then used to perform probabilistic tractography. Inflated ROIs derived from the resting state analysis (see above; produced from *3dROIMaker*) were transformed from the Montreal Neurological Institute (MNI) space (Ashburner and Ridgway, 2013) of the resting state data to the diffusion-weighted space, for tractography analysis. Next, *3dTrackID* (Taylor and Saad, 2013) was applied to produce an intensity map of probabilistic connections with the following settings for all datasets: FA > 0.15; turning angle < 50°, N_{seed} = 5 tract seeds per voxel; N_{mc} = 1000 Monte Carlo iterations and a fractional threshold of f_{tr} = 0.05 (so that f_{tr} x N_{seed} x N_{MC} = 250 tracts/voxel). *3dTrackID* (Taylor & Saad, 2013) also generated the number of streamlines (fiber count) and anatomical distances between region pairs. The number of streamlines was then used to calculate the strength of connectivity between each pair of ROIs as a part of the *awFC* technique (refer to Ayyash et al. (2021)). To reduce the tractography distance bias, a Poisson regression-based adjustment was performed: $\log(\mu(Sij|gij) = \alpha_0 + \alpha_1 g_{ij}$, where $g_{ij}$is the distance between each region pair, $S_{ij}$is the unbiased number of streamlines, α_1 is the bias adjustment factor. The number of streamlines between region pairs was corrected accordingly. Functional Connectivity between brain regions can be supported by either direct or indirect SC (Honey et al., 2009; Teipel et al., 2010). To incorporate indirect connections into the SC measure, the following was applied: π_{ij}=max[π_{ij}, $\max_m(\pi_{im}\pi_{mj})$], where π are the probabilities of SC, i is the starting ROI, j is the target ROI, and m is the third connection.

2.9. awFC analysis

Once the FC and SC values between ROIs in each network were estimated, FC data and weighted SC data were fused together using the *awFC* technique (Refer to (Ayyash et al., 2021) for the pipeline details). The functional and structural dissimilarity matrices were computed and constructed for each ROI pair within each network for each participant. Dissimilarity was calculated for each ROI pair by one minus connectivity similarity (functional dissimilarity, one minus FC; structural dissimilarity, one minus SC). Data fusion was calculated using the formula: $d_{ij} = w_{ij} \bullet f_{ij}$, where d_{ij} is a combined dissimilarity measure, w_{ij} is structural dissimilarity and f_{ij} is functional dissimilarity. Next, we used the d_{ij} to calculate the *awFC* metric: $awFC = 1 - |d_{ij}|$. In the current study we examined *awFC* between ROI pairs for (1) REM and NREM at baseline, (2) REM and NREM at week-8, (3) REM at baseline and REM at week-8, within each ROI pair for every RSN using a Mann-Whitney U test. Effect sizes were calculated using Cohen's *d* (Cohen, 1998).

2.10. Group analyses using R

The normality of the awFC data for REM and NREM participants was tested using the Shapiro-Wilk test ($p < 0.05$). However, the these data did not satisfy normality and as a result, a Mann-Whitney test was conducted. Mann-Whitney U tests were performed in each of the 3-paired comparisons (REM versus NREM at baseline; REM versus NREM at week-8; REM at baseline versus week-8). The significance threshold for comparisons was set at $p < 0.05$. To account for multiple comparisons, p-values were adjusted by controlling for the False Discovery Rate (FDR) using the Benjamini-Hochberg procedure. We only report the results that survive the FDR correction for multiple testing ($p_{adj} < 0.05$).

2.11. Associations of cognitive variables to awFC using principal component analysis and principal component regression

RSNs *awFC* may be related to cognitive and behavioural changes in MDD at remission. We explored the relationship between *awFC* and cognitive variables in each region pair at the level of $p < 0.05$. Associations were explored only for regions with significant *awFC* differences between REM and NREM groups.

Five cognitive variables of the CNS-VS test were explored: memory, cognitive flexibility, complex attention, processing speed and neurocognitive index. Multicollinearity among these variables was assessed

with Pearson correlation using the *ggpairs* function from the *GGally* package in R (Schloerke et al., 2018), which identified that significant correlations existed between the five cognitive variables [See Supplementary Fig. 1]. Variables that are correlated are considered redundant, thus a PCA can be applied to reduce the redundancy (Kassambara, 2017; Refaat, 2010). The Principal components produced from the PCA are orthogonal and uncorrelated to one another (Hair et al., 2009). PCA was performed with the R package (R Core Team, 2018) using the *princomp* function. A PCA was applied to the five cognitive variables and visually displayed using the *fviz_pca_var* function, from the "factoextra package" (Kassambara, 2017). It was considered sufficient to retain one component from PCA to interpret the data, if they met the following criteria: (1) Principal components (PCs) having an eigenvalue greater than one (Jackson, 1993) (2) PCs corresponding to a minimum of 60% explained variance from the data] (3). Graphically, components observed before the first 'elbow' of the Scree plot were retained. [Refer to Supplementary Fig. 1]. The output of PCA (PCs) was used as an input (independent variables) for Principal Component Regression (PCR). A linear mixed effects regression was performed, whereby the PCs, MADRS, age and sex were taken to be the explanatory variables and *awFC* was taken to be the outcome variable. A two-level factor (REM and NREM) interaction effect was included in the mixed effects model. To account for possible site bias in the data, participants nested within-site were included as a random effect. Principal component regression (PCR) was applied using the *lme* function from the *nlme* package in R (R Core Team, 2018). For each region pair within a network, PCs with significant associations with the *awFC* were post-hoc tested. Interpretation of the PCs can be made by examining the component loadings (Hair et al., 2009). The component loadings are computed correlations between the original variables and the PCs (Hair et al., 2009). A variable was considered significantly loaded on a PC with a cut-off absolute threshold correlation of 0.3 (Hair et al., 2009). The most important variables (high loadings on PCs) were identified to perform multiple linear regression models to further explore the association between the original variables (with the highest loadings on each PC), and the outcome variable (*awFC*).

Post-hoc analyses were carried out only for significant ROI-pairs within RSNs. Three separate analyses were conducted using multiple linear regression analysis. The significant regions pairs were assessed for the following groups: (1) REM and NREM at baseline, (2) REM and NREM at week-8, (3) REM at baseline and REM at week-8. For the first analysis, the association between cognitive variables at week-8 and *awFC* at week-8 were assessed using PCA/PCR. The second analysis explored the association between the change in cognitive variables (from baseline to week-8) and change in *awFC* (from baseline to week-8) using PCA/PCR. The third analysis evaluated the association between the change in cognitive variables (from baseline to week-8) and *awFC*, at baseline. Changes in *awFC* were calculated by subtracting the post-treatment (week-8 *awFC*) from the pre-treatment (baseline *awFC*) connectivity values, change in MADRS was calculated by subtracting the baseline MADRS from the week-8 MADRS as previously described (Persson et al., 2020).

3. Results

3.1. Participants in the analysis

MADRS scores were used to assess depression severity and to define remission status. We defined REM as participants that had a MADRS score ≤ 10 at week-8, that was maintained at week-16 of treatment (Hawley et al., 2002; Mendlewicz, 2008), whereas participants with a MADRS score > 10 at week-8 and who maintained a > 10 score at week-16 (after 8 weeks of adjunctive treatment with aripiprazole) were labeled as NREM. This study focused exclusively on imaging data from the REM and NREM participants at baseline and week-8.

From the 211 participants in the CAN-BIND-1 study, 147 met the inclusion criteria for REM or NREM. Further additional participants were removed from this sample as the result of excessive motion in the scanner (n = 21) or missing rsfMRI or DTI imaging data at baseline (n = 16) or at week-8 (n = 18). This resulted in the exclusion of 23 REM and 31 NREM, leaving 93 participants (66 NREM and 27 REM) retained for this analysis.

3.2. Demographics

Table 1 summarizes the demographic characteristics and provides medical history of antidepressants for the participants in each group belonging to: REM and NREM.

3.3. ROIs Defined Within RSNs

The results shown are for group-wise parcellation obtained from the REM and NREM groups. Table 2 lists the volume, anatomical names and locations of each group of ROI within each RSN.

3.4. Anatomically Weighted Functional Connectivity Group Comparisons

The Wilcoxon-test showed a significant difference in *awFC* between groups. Fig. 1 illustrates the ROI pairs with statistically significant connectivity differences between REM and NREM groups at $p_{adj} < 0.05$ (FDR corrected). Our results revealed group differences predominantly in the comparison between REM and NREM at week-8 in all networks except the LIM. There was also a connectivity difference identified for REM at baseline compared to REM at week-8 within the DAN. However, no group differences in connectivity were detected when comparing the REM to the NREM at baseline. These results are summarized in Table 3. In addition, as a reference, separate analyses were performed for SC and FC between each ROI pair within each RSN. Table 4 illustrates group-level comparison of FC and SC for each *awFC* comparison.

Group Comparisons at Week 8: Comparing connectivity within RSNs for REM and NREM at week-8, revealed connectivity differences in the DMN, FPN, VAN, and DAN. Table 5 contains a summary of the mean and standard error of network nodal connections with significantly different *awFC* for each group. Results showed that the *awFC* was significantly lower in the REM as compared to NREM at week-8 in the DMN: between nodes linking the a) middle prefrontal cortex and the left middle

Table 1
Demographic Characteristics.

Characteristic	Non-Remitters, N = 66[1]	Remitters, N = 27[1]	p-value[2]
Sex			0.711
Female	44 (66.7%)	17 (63.0%)	
Male	22 (33.3%)	10 (37.0%)	
Age in years Mean (SD)	33 (12)	34 (11)	0.402
MADRS Mean (SD)	21 (8)	5 (3)	**< 0.001** *
Education, years Mean (SD)	17 (2)	17 (4)	0.724
Age of Onset of MDD, years Mean (SD)	19 (7)	19 (9)	0.731
Duration of Current MDE, Months			0.801
≤ 12 months	35 (53.0%)	14 (51.9%)	
1-2 years	8 (12.1%)	2 (7.4%)	
> 2 years	19 (28.8%)	9 (33.3%)	
Other	4 (6.1%)	2 (7.4%)	
Number of MDE's Mean (SD)	4 (3)	5 (3)	
Antidepressants			
Drug Naive	33 (50.0%)	11 (40.7%)	
Past History of Antidepressants	33 (50.0%)	16 (59.3%)	

[1] n (%); Mean (SD)
[2] Pearson's Chi-squared test; Wilcoxon rank sum test; Fisher's exact test
*Bonferroni correction for multiple testing
Note: N = Number of participants, SD = Standard Deviation, MDD = Major Depressive Disorder, MDE = Major Depressive Episode, MADRS = Montgomery-Asberg Depression Rating Scale.

Table 2
Summarized characteristics of all the brain regions within each resting-state network. The volume (number of voxels), centroid location in MNI co-ordinates and anatomical names of each regions of interest (ROIs) are listed. ROIs were defined using FATCATs *3dROIMaker* command.

ROI no.	Anatomical location	Peak MNI coordinates x y z			Volume (# of voxels)
DEFAULT MODE NETWORK					
1	Left middle temporal gyrus	-62	-22	-16	55
2	Middle prefrontal cortex	-2	54	8	55
3	Posterior cingulate cortex/Precuneus	-2	-54	28	55
4	Left angular gyrus	-50	-62	28	55
FRONTOPARIETAL NETWORK					
5	Left cerebellum	-34	-70	-40	45
6	Right orbitofrontal gyrus	42	54	-8	10
7	Right middle frontal gyrus	34	14	56	45
8	Right angular gyrus (lateral occipital cortex)	50	-54	44	45
9	Paracingulate gyrus	6	34	36	10
LIMBIC NETWORK					
10	Right parahippocampal gyrus, amygdala, hippocampus, temporal fusiform cortex	30	-6	-40	37
11	Lingual gyrus	-6	-94	-4	37
12	Paracingulate gyrus	2	10	52	37
VENTRAL ATTENTION NETWORK					
13	Left insular cortex (frontal operculum cortex)	-38	10	0	80
14	Right insular cortex (frontal operculum cortex)	42	14	-8	80
15	Anterior cingulate gyrus, paracingulate gyrus	-6	22	32	80
16	Left middle frontal gyrus	-30	46	20	80
DORSAL ATTENTION NETWORK					
17	Right and left postcentral gyrus	-42	-34	44	100
18	Left parahippocampal gyrus (anterior and posterior), lingual gyrus, temporal fusiform gyrus	-26	-26	-20	40
19	Right insular cortex	42	-2	8	36
20	Right precentral gyrus	58	10	24	100
21	Superior frontal pole, paracingulate gyrus	6	54	12	65

temporal gyrus (See Fig. 2a); b) the left angular gyrus and the left middle temporal gyrus (see Fig. 2b); c) between the left angular gyrus to middle prefrontal cortex (see Fig. 2c). There were also significantly lower *awFC* values within the FPN between regions of the left cerebellum and the right orbitofrontal gyrus for the REM compared with NREM at week-8 (Fig. 2d). In addition, lower connectivity values were found in the VAN for the REM compared to NREM at week-8 between the right insular cortex and the left middle frontal gyrus (Fig. 2e) and between anterior cingulate gyrus and the left middle frontal gyrus (Fig. 2 f).

Group Comparisons Examining Change from baseline to Week 8: Within group comparisons examining the connectivity changes associated with a positive medication response identified significantly greater *awFC* connectivity in the DAN between the pre-central and post-central gyrus and weaker connectivity in the FPN between the left cerebellum and right orbitofrontal gyrus. (Fig 3 g and 3 h).

4. Cognitive variables associated with awFC

4.1. Principal component analysis

PCA was performed on five cognitive variables (processing speed, memory, cognitive flexibility, complex attention and neurocognitive index), which revealed one significant PC with an eigenvalue>1 (eigenvalue $= 3.34$) and accounted for 63.8% of the total variance in the data [See Supplementary Fig. 1]. Significant associations were found with the outcome variable *awFC* in the FPN between the right medial frontal gyrus and the left cerebellum. Processing speed was the highest contributor to the first PC, followed by memory, cognitive flexibility, neurocognitive index and complex attention (a total of five PCs).

4.2. Principal component regression

PCR was then performed for the RSNs to examine *awFC* differences between groups for each ROI-pair. The PCR included *awFC* as the outcome variable and the first PC, MADRS, age and sex as independent variables. In addition, random effects (participants nested within-site) were included. To further investigate which cognitive variable was driving the effect for the PCs, separate analyses were conducted for each group comparison, correlating *awFC* in different groups (at baseline, week-8 and from baseline to week-8) with cognitive variables and MADRS.

4.3. Baseline awFC Associations with cognitive variables

After performing a PCA [see **Principal Component Analysis** section**]**, a PCR was performed to examine associations between the first PC (among five PCs) and the *awFC* at baseline. We did not observe a significant association between the first PC and awFC.

4.4. Association of week-8 cognitive variables with week-8 awFC

After performing a PCA [see see PCA section**]**, a PCR was performed to examine associations between the first PC (among five PCs) and the *awFC* at week 8. We found a significant association between the first PC and *awFC* ($p_{adj} = 0.01$), which prompted further analysis to investigate which cognitive variables contributed to this effect. Multiple linear regressions were performed examining each cognitive variable and *awFC*. The post-hoc regression revealed that brain connectivity between the left cerebellum to the right orbitofrontal gyrus was associated with cognitive flexibility ($p_{adj} = 0.0011$), and neurocognitive index ($p_{adj} = 0.021$) for the week-8 NR.

4.5. Changes in awFC in association with changes in cognitive variables

After performing a PCA (see PCA section**)**, a PCR was conducted to assess the association between the first PC (among five PCs) and the changes in awFC from baseline to week-8 (calculated by subtracting week-8 *awFC* from baseline *awFC*). No significant associations were identified between the first PC and changes in awFC.

5. Discussion

To our knowledge, this is the first study to combine fMRI and DTI in a fused manner to assess medication response in MDD, while simultaneously comparing these results to traditional FC and SC indices. The current study investigated *awFC* in MDD in five RSNs (the DMN, FPN, DAN, VAN, and LIM), with the aim of identifying differences between a) baseline and week-8 for the REM group, b) REM and NREM at baseline prior to the initiation of medication therapy, and c) REM and NREM following 8 weeks of treatment with the SSRI, escitalopram. Using the *FATCAT-awFC* pipeline (Ayyash et al., 2021), we identified differences in connectivity strength in four of five RSNs examined. Within group differences for REM were observed between the baseline period and week-8, and revealed REM at week-8 to have increased *awFC* across time within the DAN between the right and left post central gyrus to right precentral gyrus. In the comparison at baseline between REM and NREM no significant group differences were identified among the five RSNs. This finding is similar to reports in the literature using rsfMRI analysis, where there were no signs of group differences at baseline between REM and NREM (Wang et al., 2014). However, we did find group differences, particularly reductions in *awFC* at 8 weeks for the REM compared to NREM across different RSNs including the: DMN, FPN and VAN. Our findings are consistent with observations that in MDD, response to

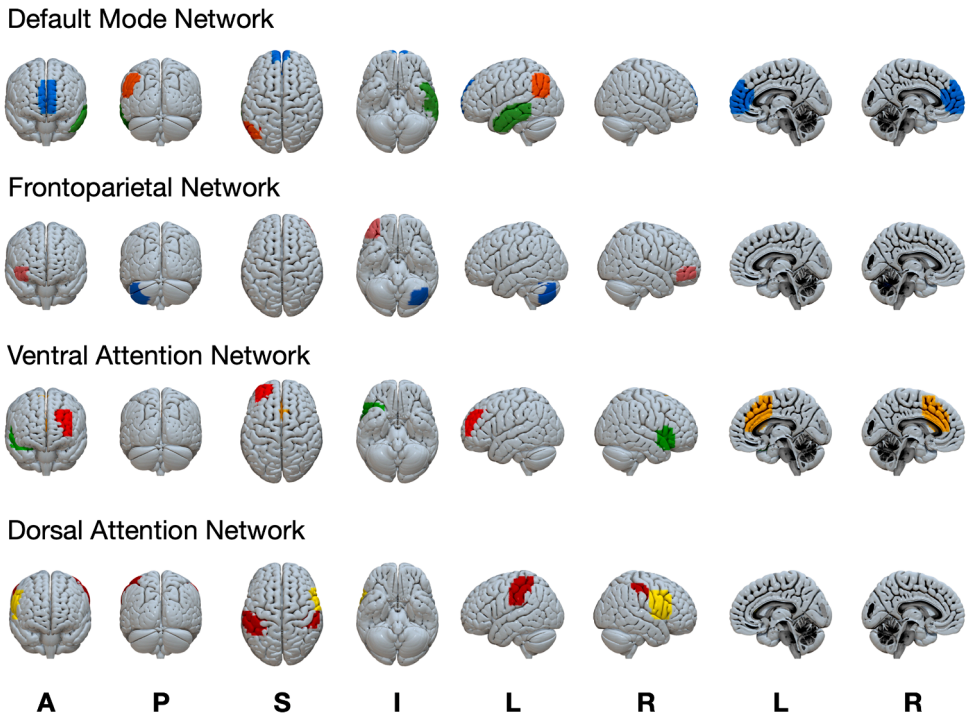

Fig. 1. Group differences in anatomically weighted functional connectivity are displayed for each network. Isolated brain regions were defined using the FATCAT command *3dROIMaker*. Each colour represents a different ROI for each network; Default Mode Network, blue ROI= middle prefrontal cortex, green ROI = left middle temporal gyrus, orange ROI= left angular gyrus; Frontoparietal Network, brown ROI = right orbitofrontal gyrus, blue ROI = left cerebellum; Ventral Attention Network, red ROI= left middle frontal gyrus, green ROI = right insular cortex, orange ROI = anterior cingulate gyrus/paracingulate gyrus; Dorsal Attention Network, red ROI = right and left postcentral gyrus, yellow ROI = right precentral gyrus. ROI = region of interest, Anatomical positions, A = anterior view, P = posterior view, S = superior view, I = inferior view, L = left view, R= right view.

Table 3
Anatomically weighted functional connectivity (*awFC*) was compared between groups using a Wilcox-test. Displayed are the significant differences of *awFC* measures between brain regions for: remitters vs non-remitters at baseline, remitters vs non-remitters at week8, and remitters at baseline vs remitters at week8.

Start ROI	End ROI	COMPARISON		
		REM vs NREM (baseline)	REM vs NREM (week-8)	REM (baseline) vs REM (week8)
DEFAULT MODE NETWORK				
L-MTG	MPFC	1.00	0.0050 *	0.037 *
L-MTG	L-AG	1.00	0.0051 *	0.108
MPFC	L-AG	1.00	0.014 *	0.093
FRONTOPARIETAL NETWORK				
L-CER	R-OFG	0.921	0.008 *	0.005 *
VENTRAL ATTENTION NETWORK				
R-INS	L-MFG	0.802	0.021 *	1.00
ACC/PCG	L-MFG	0.901	0.027 *	1.00
DORSAL ATTENTION NETWORK				
R+L Post CG	R-Pre CG	0.457	1.00	0.005 *

**p-value* (FDR corrected) < 0.05, REM = remitters, NREM = non-remitters, ROI = region of interest, L-MTG = left middle temporal gyrus, MPFC = middle prefrontal cortex, L-AG = left angular gyrus, L-CER = left cerebellum, R-OFG = right orbitofrontal gyrus, R-INS = right insular cortex, ACC/PCG = anterior cingulate cortex, L-MFG = left middle frontal gyrus, R+L Post CG = right and left postcentral gyrus, right Pre CG = right precentral gyrus

medication is accompanied not only by increased connectivity within the executive control network (i.e. pre and post central gyrus) brain regions longitudinally (within group REM from baseline to week 8) (Karim et al., 2017), but also, by reductions in connectivity following treatment for REM (compared to NREM) between several brain regions

Table 4
Structural connectivity, functional connectivity and anatomically weighted functional connectivity were compared between groups using a Wilcoxon-test. Regions where anatomically weighted functional connectivity was significant for: remitters at week-8 compared to NREM at week-8 and REM at baseline compared to remitters at week-8 - and their corresponding structural and functional connectivity significance is shown.

Start ROI	End ROI	SC p-value (FDR corrected)	FC p-value (FDR corrected)	*awFC* p-value (FDR corrected)
Remitters at week-8 compared to non-remitters at week-8				
DEFAULT MODE NETWORK				
L-MTG	MPFC	1.00	0.0051 *	0.0050 *
L-MTG	L-AG	0.00815 *	0.005 *	0.0051 *
MPFC	L-AG	0.960	0.015 *	0.014 *
FRONTOPARIETAL NETWORK				
L-CER	R-OFG	0.980	0.0095 *	0.008 *
VENTRAL ATTENTION NETWORK				
R-INS	L-MFG	0.370	0.023 *	0.021 *
ACC	L-MFG	0.310	0.030 *	0.027 *
Remitters at baseline compared to remitters at week-8				
DORSAL ATTENTION NETWORK				
R+L Post CG	R-Pre CG	1.00	0.009	0.005 *
DEFAULT MODE NETWORK				
L-MTG	MPFC	1.00	0.037	0.037
FRONTOPARIETAL NETWORK				
L-CER	R-OFG	0.05 *	0.009 *	0.005 *

**p-value* (FDR corrected) < 0.05. ROI = region of interest, SC = structural connectivity, FC = functional connectivity, *awFC* = anatomically weighted functional connectivity, FDR = false discovery rate, L-MTG = left middle temporal gyrus, MPFC = middle prefrontal cortex, L-AG = left angular gyrus, L-CER = left cerebellum, R-OFG = right orbitofrontal gyrus, R-INS = right insular cortex, ACC/PCG = anterior cingulate cortex, L-MFG = left middle frontal gyrus, R+L Post CG = right and left postcentral gyrus, right Pre CG = right precentral gyrus

Table 5
Anatomically weighted functional connectivity (*awFC*) was compared between groups using a Wilcoxon-test. ROI-pair connectivity metrics: mean, standard error and effect size for remitters at week-8 compared to non-remitters at week-8 and remitters at baseline compared to remitters at week-8 are displayed. Only the ROI-pairs with significant connectivity differences between groups are listed. The effect sizes were determined using Cohen's d and reported.

Start ROI	End ROI	REM at Week-8 (Mean ± SE)	NREM at Week-8 (Mean± SE)	Effect size (Cohen's *d*)
Remitters at week-8 compared to non-remitters at week-8				
DEFAULT MODE NETWORK				
L-MTG	MPFC	0.35± 0.064	0.53 ± 0.034	0.60 (medium)
L-MTG	L-AG	0.45± 0.049	0.60 ± 0.031	0.56 (medium)
MPFC	L-AG	0.44 ± 0.053	0.60 ± 0.029	0.61 (medium)
FRONTOPARIETAL NETWORK				
L-CER	R-OFG	0.056± 0.045	0.22 ± 0.036	0.59 (medium)
VENTRAL ATTENTION NETWORK				
R-INS	L-MFG	0.21± 0.061	0.40 ± 0.031	0.69 (medium)
ACC	L-MFG	0.39 ± 0.054	0.54 ± 0.022	0.71 (medium)
Remitters at baseline compared to remitters at week-8				
Start ROI	**End ROI**	**REM at Baseline (Mean ± SE)**	**REM at Week-8 (Mean ± SE)**	**Effect size (Cohen's d)**
DORSAL ATTENTION NETWORK				
R+L Post CG	R-Pre CG	0.26± 0.034	0.39 ± 0.047	0.63 (medium)
DEFAULT MODE NETWORK				
L-MTG	MPFC	0.527 ± 0.038	0.358 ± 0.062	0.13 (negligible)
FRONTOPARIETAL NETWORK				
L-CER	R-OFG	0.22 ± 0.038	0.046± 0.044	0.923 (large)

REM = remitters, NREM = non-remitters, ROI = region of interest, SE = standard error, L-MTG = left middle temporal gyrus, MPFC = middle prefrontal cortex, L-AG = left angular gyrus, L-CER = left cerebellum, R-OFG = right orbitofrontal gyrus, R-INS = right insular cortex, ACC/PCG = anterior cingulate cortex, L-MFG = left middle frontal gyrus, R+L Post CG = right and left postcentral gyrus, right Pre CG = right precentral gyrus

(Xiao et al., 2019), a change that may reflect a normalisation of previously aberrant neural activities (Aizenstein et al., 2014; Xiao et al., 2019). Our findings suggest that utilizing our *FATCAT-awFC* pipeline, we can detect and distinguish connectivity differences associated with medication response and nonresponse.

5.1. Remitters at baseline compared to week-8: within group differences in RSN connectivity

In order to examine the brain connectivity changes that occur as a result of a favourable response to medication, we examined within-group connectivity for REM from baseline to week-8.

5.2. Dorsal attention network

We identified stronger *awFC* in the DAN between the right precentral gyrus and both the right and left post-central gyri (components of the executive control network) for REM at week-8 relative to REM at baseline. These findings are like those of Karim et al. (2017), who found that participants with late-life depression administered antidepressants (venlafaxine in the first phase, followed by aripiprazole in second phase) showed increased FC between the executive control network and the right precentral gyrus in week-12 REM relative to REM at baseline (Karim et al., 2017). These findings suggest that a positive response to antidepressant medication is associated with increases in connectivity across brain regions responsible for cognitive control, goal-directed behaviors and working memory (Menon and Uddin (2010)).

5.3. Frontoparietal network

Lower connectivity was found in REM at week-8 compared to the REM at baseline within the FPN, between regions in the right orbitofrontal gyrus and in the left cerebellum. Interestingly, the REM at week-8 also showed decreased connectivity, compared to NREM at week-8 [See 'Remitters at Week-8 compared to Non-Remitters at Week-8: Group Differences in RSNs' for more discussion]. These finding may reflect a "normalization" of function and connectivity in patients that responded favourably to antidepressant medication (Xiao et al., 2019). This idea of a shift toward normalization offers new insight into the brain changes associated with a positive response to medication.

5.4. Remitters at week-8 compared to non-remitters at week-8: group differences in RSNs

In order to examine the connectivity changes distinguishing Remitters from Non-Remitters following a course of antidepressants we contrasted the awFC findings for REM with that of NREM participants at 8 weeks.

5.5. Default mode network

We observed significantly lower *awFC* within the DMN for REM as compared to NREM at week-8 in three ROI-pairs within the DMN, including the a) middle prefrontal cortex (PFC) to the left middle temporal gyrus, b) left middle temporal gyrus to the left angular gyrus, and c) left angular gyrus to medial prefrontal cortex. These findings are similar to other studies in the reported literature identifying that antidepressant treatment of MDD results in reduced connectivity between brain regions within the DMN. For instance, a study by Xiao et al. (2019) found MDD participants who reached a rapid remission (5 days), displayed reductions in FC between nearly all DMN ROIs compared to unmedicated MDD participants. These authors suggested that a possible explanation for the reductions in DMN connectivity strength for MDD remitters may be a medication induced normalization of the hyperconnectivity of the DMN (Xiao et al., 2019). Support this framework can be found in a study by Karim et al. (2017), which found that week-12 Late-life MDD remitters were characterized by decreased FC in the DMN between the right inferior frontal gyrus and the supramarginal gyrus (Karim et al., 2017). Taken together, our findings suggest that the response to SSRIs in MDD may be associated with joint FC and SC reductions within DMN brain regions.

5.6. Frontoparietal network

Reduced connectivity was also found in the REM at week-8 compared to the NREM at week-8 within the FPN, between regions in the right orbitofrontal gyrus and the left cerebellum. These findings are consistent with those of Lisiecka et al. (2011), who performed a task-based fMRI study to assess the FC changes following antidepressant treatment. In their study, increased FC between the orbitofrontal cortex and the cerebellum was observed in patients who did not reach remission with antidepressant treatment (Lisiecka et al., 2011). They concluded that increased connectivity between the orbitofrontal gyrus and the cerebellum was reflective of a more persistent depression, rather than a more severe form of depression (Lisiecka et al., 2011). Interestingly, we found higher *awFC* in the NREM at week-8 compared to the REM at week-8. These results demonstrate that lower *awFC* within the FPN may be reflective of remission status.

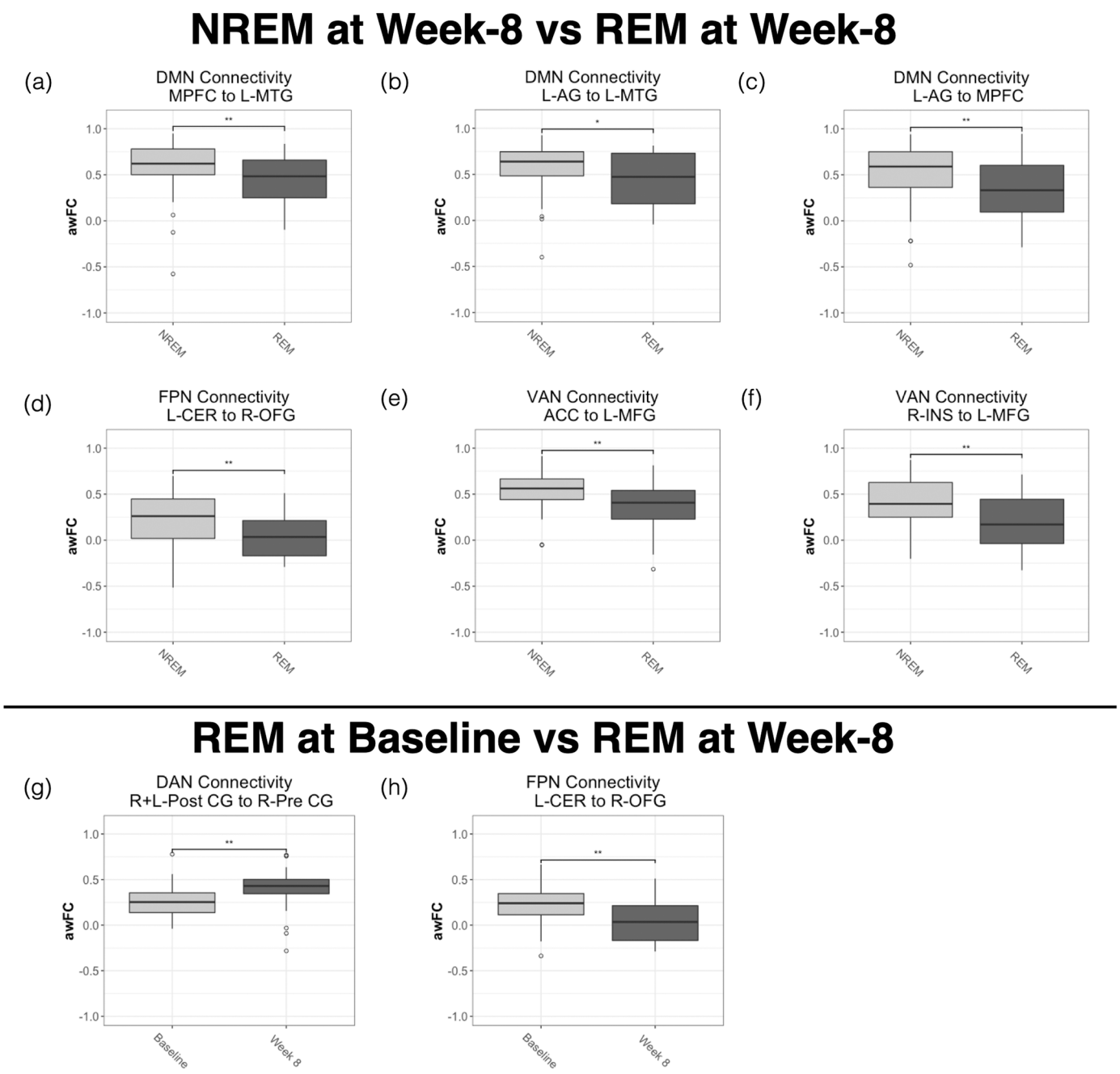

Fig. 2. Boxplots of the anatomically weighted functional connectivity comparing: (a-f) – remitters at week-8 (dark gray boxes) versus non-remitters at week-8 (light gray boxes) and (g-h) remitters at baseline (light gray box) versus remitters at week-8 (dark gray box). Only ROI pairs that demonstrated significant anatomically weighted functional connectivity differences are displayed. Circles represent outliers. Note: DMN = default mode network, FPN = frontoparietal network, VAN = ventral attention network, DAN = dorsal attention network, M-PFC = middle prefrontal cortex, L-Middle Temp = left middle temporal gyrus, L-AG = left angular gyrus, L-CER = left cerebellum, R-OFG = right orbitofrontal gyrus, R-AG = right angular gyrus, R-INS = right insular cortex, L-middle frontal = left middle frontal gyrus, L-middle frontal = left middle frontal gyrus, ACC = anterior cingulate cortex, R+L-Post CG= right and left post central gyrus, R-Pre CG = right pre-central gyrus.

5.7. Ventral attention network

In this study, we observed weaker connectivity in REM compared with NREM at week-8 between two region pairs (a) between the insula and the middle frontal gyrus, and (b) between the anterior cingulate cortex and the middle frontal gyrus. In a similar study to ours, Karim et al. (2017) carried out rsfMRI and examined medication response in MDD. They found that REM participants had weaker functional connectivity between the inferior frontal gyrus and the middle frontal gyrus compared to the NREM participants (Karim et al., 2017). Furthermore, in an implicit emotion processing task based fMRI study done by Godlewska et al. (2016), MDD participants were identified as REM or NREM based on their response following 6 weeks of escitalopram treatment. Participants' neural response to emotional faces was examined early in the course of treatment, after the initial 7 days of medication therapy (Godlewska et al., 2016). Responders to escitalopram, compared to non-responders, showed greater reductions in the neural activation of the insula and the dorsal anterior cingulate during the processing of negative fearful faces (Godlewska et al., 2016). Similar to the DMN, we found the VAN to also have reduced connectivity in the REM compared

to NREM. Additionally, our findings are consistent with functional imaging findings identifying that response to escitalopram treatment is associated with the overall pattern of reduced connectivity in the VAN (Li et al., 2021).

5.8. Contribution of traditional FC and traditional SC in the analysis of *awFC*

The traditional SC and traditional FC were performed to allow the visual comparison of significant group differences. Their combination at times allowed for a more significant connectivity measure, while at other times it performed only as well as the traditional FC alone. This is the basic principle behind the original *awFC* technique. While the *awFC* measure appears to predominantly be driven by FC, there are times that connectivity differences were supported by SC as well. At times, the significance level for group differences was amplified (i.e. DAN), even in the absence of significant SC group differences. This may perhaps be due to the adjusted SC distance bias, and consideration of indirect structural connections between brain regions.

5.9. Associations between cognitive variables and awFC

The significant association between cognitive variables collected at week-8, and *awFC* at week-8 (within the FPN between the right orbitofrontal gyrus and left cerebellum) was reported for the NR. An increase in *awFC* was found to reflect an increase in cognitive flexibility, and neurocognitive index, between the left cerebellum and the right orbitofrontal gyrus. This brain region was found to be associated with cognitive flexibility and neurocognitive index as measured by the CNS-VS at week-8 in this study.

Previous studies have found that the orbitofrontal cortex (Boulougouris et al., 2007) and the cerebellum (De Bartolo et al., 2009) mediate cognitive flexibility. Previous studies have shown that cerebellar (De Bartolo et al., 2009) and orbitofrontal lesions (Robbins et al., 2012) impact cognitive flexibility. The cerebellum may play a role in monitoring incoming sensory information (i.e. from the orbitofrontal gyrus) and navigate appropriate behaviour (i.e. motor movements) based on environmental conditions (Bower, 2002; Ito, 2002; Schmahmann, 2004; Thach, 2007).

5.10. Limitations

One limitation we encountered in our previous work (Ayyash et al., 2021), concerned the observation that ROIs could encroach on each other, overlapping across shared borders, and this may have impacted the overall connectivity values. We addressed this limitation in the present study by using ROIs that were smaller in size. However, in a combined FC-SC analysis, such as this study, smaller ROIs can result in a greater effect size for the FC component. Furthermore, the use of smaller ROIs made it necessary to inflate the ROI boundaries so that during the DTI analysis the initial seed points fell in white matter and could be detected. As a consequence, this may have reduced the accuracy of the SC parameters. Future work will need to find the best trade-off between the optimal ROI size and the optimal amount of ROI inflation to set white matter seeds.

Finally, while our differentiation between clinical groups may meet the recent sample size recommendations for neuro-imaging only analyses (Non-Remitters N = 66; Remitters N = 27; see Marek et al., 2022), we fall far short of the 1000 s recommended for brain wide association studies where associations are drawn between inter-individual variability in human brain structure/function and psychiatric symptomatology or cognition (Marek et al., 2022). This research, therefore, should be considered preliminary work that may help guide future research involving larger study groups and our extrapolation to cognitive variables considered in need of further replication.

5.11. Future directions

In this paper we examined changes in anatomically weighted functional connectivity in individuals with MDD identified as REM or NREM following a course of SSRI medication escitalopram. Future studies could investigate treatment-resistant depression and the effects of different classes of medication on brain connectivity changes. In addition, it would be of interest to investigate the use of diffusion spectrum imaging (DSI) in our pipeline instead of DTI, as it is capable of delineating tracts in complex and multidirectional areas (i.e. crossing fibers, small fibers) more accurately. This will be beneficial for our pipeline, as the *FATCAT-awFC* approach uses tract count to quantify SC, and DSI is capable of assessing tract count with greater sensitivity (Bassett et al., 2011).

6. Conclusion

We have found that the combination of structural and functional connectivity can be achieved using a relatively straight forward pipeline and that the application of these tools can help identify connectivity differences that distinguish depressed patients that will demonstrate a positive therapeutic response to the SSRI escitalopram from those who do not. We used the *FATCAT-awFC* analysis approach to investigate the connectivity changes within five RSNs (DMN, FPN, DAN, VAN, LIM) for patients with MDD who matched criteria for REM or NREM after 8 weeks of treatment with the SSRI escitalopram. The results identified that treatment outcome was reflected in *awFC* differences between REM and NREM within four of the five RSNs. Further, the observed increased connectivity from baseline to week-8 in the DAN, and decreased connectivity from baseline to week-8 in the FPN, were suggested to reflect the treatment propagated normalisation of the aberrant connectivity associated with MDD. Finally, cognitive variables were found to be associated with *awFC* for one region pair in the FPN. This suggested that altered connectivity of the orbitofrontal gyrus and cerebellum may have played a role in the deficits in cognitive flexibility for non-remitted MDD participants.

Acknowledgements

CAN-BIND is an Integrated Discovery Program carried out in partnership with, and financial support from, the Ontario Brain Institute, an independent non-profit corporation, funded partially by the Ontario government. The opinions, results and conclusions are those of the authors and no endorsement by the Ontario Brain Institute is intended or should be inferred. All study medications were independently purchased at wholesale market values.

We would like to thank Keith Ho for his help with organizing the clinical data, and all the patients, controls, and health care workers involved in this project for the generous contribution of their time and their participation in this work.

Appendix A. Supporting information

Supplementary data associated with this article can be found in the online version at doi:10.1016/j.ibneur.2023.12.011.

References

Abo Aoun, M., P Meek, B., Modirrousta, M., 2019a. Cognitive profiles in major depressive disorder: comparing remitters and non-remitters to rTMS treatment. Psychiatry Res. 279, 55–61. https://doi.org/10.1016/j.psychres.2019.07.007.

Aizenstein, H.J., Khalaf, A., Walker, S.E., Andreescu, C., 2014. Magnetic resonance imaging predictors of treatment response in late-life depression. J. Geriatr. Psychiatry Neurol. 27 (1), 24–32. https://doi.org/10.1177/0891988713516541.

Albert, K.M., Potter, G.G., Boyd, B.D., Kang, H., Taylor, W.D., 2019. Brain network functional connectivity and cognitive performance in major depressive disorder. J. Psychiatr. Res. 110, 51–56. https://doi.org/10.1016/j.jpsychires.2018.11.020.

Ashburner, J., Ridgway, G.R., 2013. Symmetric diffeomorphic modeling of longitudinal structural MRI. Front. Neurosci. 6 https://doi.org/10.3389/fnins.2012.00197.
Ayyash, S., Davis, A.D., Alders, G.L., MacQueen, G., Strother, S.C., Hassel, S., Zamyadi, M., Arnott, S.R., Harris, J.K., Lam, R.W., Milev, R., Müller, D.J., Kennedy, S.H., Rotzinger, S., Frey, B.N., Minuzzi, L., Hall, G.B., Investigator Team, C. A.N.-B.I.N.D., 2021. Exploring brain connectivity changes in major depressive disorder using functional-structural data fusion: A CAN-BIND-1 study. Hum. Brain Mapp. https://doi.org/10.1002/hbm.25590.
Ballenger, J.C., 1999. Clinical guidelines for establishing remission in patients with depression and anxiety. J. Clin. Psychiatry 60 (*Suppl 22*), 29–34.
Bassett, D.S., Brown, J.A., Deshpande, V., Carlson, J.M., Grafton, S.T., 2011. Conserved and variable architecture of human white matter connectivity. NeuroImage 54 (2), 1262–1279. https://doi.org/10.1016/j.neuroimage.2010.09.006.
Bhalla, R.K., Butters, M.A., Mulsant, B.H., Begley, A.E., Zmuda, M.D., Schoderbek, B., Pollock, B.G., Reynolds, C.F., Becker, J.T., 2006. Persistence of neuropsychologic deficits in the remitted state of late-life depression. Am. J. Geriatr. Psychiatry: Off. J. Am. Assoc. Geriatr. Psychiatry 14 (5), 419–427. https://doi.org/10.1097/01.JGP.0000203130.45421.69.
Boulougouris, V., Dalley, J.W., Robbins, T.W., 2007. Effects of orbitofrontal, infralimbic and prelimbic cortical lesions on serial spatial reversal learning in the rat. Behav. Brain Res. 179 (2), 219–228. https://doi.org/10.1016/j.bbr.2007.02.005.
Bower, J.M., 2002. The organization of cerebellar cortical circuitry revisited. Ann. N. Y. Acad. Sci. 978 (1), 135–155. https://doi.org/10.1111/j.1749-6632.2002.tb07562.x.
Bowman, F.D., Zhang, L., Derado, G., Chen, S., 2012. Determining functional connectivity using fMRI data with diffusion-based anatomical weighting. NeuroImage 62 (3), 1769–1779. https://doi.org/10.1016/j.neuroimage.2012.05.032.
Brennan, A., Marstaller, L., Burianová, H., Benton, D., Hanley, C.J., Newstead, S., Young, H.A., 2022. Weaker connectivity in resting state networks is associated with disinhibited eating in older adults. Int. J. Obes. 46 (4), 859–865. https://doi.org/10.1038/s41366-021-01056-1.
Buckner, R.L., Krienen, F.M., Castellanos, A., Diaz, J.C., Yeo, B.T.T., 2011. The organization of the human cerebellum estimated by intrinsic functional connectivity. J. Neurophysiol. 106 (5), 2322–2345. https://doi.org/10.1152/jn.00339.2011.
Byford, S., Barrett, B., Despiégel, N., Wade, A., 2011. Impact of treatment success on health service use and cost in depression. PharmacoEconomics 29 (2), 157–170. https://doi.org/10.2165/11537360-000000000-00000.
Chaddock-Heyman, L., Weng, T.B., Kienzler, C., Erickson, K.I., Voss, M.W., Drollette, E. S., Raine, L.B., Kao, S.-C., Hillman, C.H., Kramer, A.F., 2018. Scholastic performance and functional connectivity of brain networks in children. PLOS ONE 13 (1), e0190073. https://doi.org/10.1371/journal.pone.0190073.
Churchill, N.W., Spring, R., Afshin-Pour, B., Dong, F., Strother, S.C., 2015. An automated, adaptive framework for optimizing preprocessing pipelines in task-based functional MRI. PLOS ONE 10 (7), e0131520. https://doi.org/10.1371/journal.pone.0131520.
Cipriani, A., Zhou, X., Giovane, C.D., Hetrick, S.E., Qin, B., Whittington, C., Coghill, D., Zhang, Y., Hazell, P., Leucht, S., Cuijpers, P., Pu, J., Cohen, D., Ravindran, A.V., Liu, Y., Michael, K.D., Yang, L., Liu, L., Xie, P., 2016. Comparative efficacy and tolerability of antidepressants for major depressive disorder in children and adolescents: A network meta-analysis. Lancet 388 (10047), 881–890. https://doi.org/10.1016/S0140-6736(16)30385-3.
Cochereau, J., Deverdun, J., Herbet, G., Charroud, C., Boyer, A., Moritz-Gasser, S., Le Bars, E., Molino, F., Bonafé, A., Menjot de Champfleur, N., Duffau, H., 2016. Comparison between resting state fMRI networks and responsive cortical stimulations in glioma patients. Hum. Brain Mapp. 37 (11), 3721–3732. https://doi.org/10.1002/hbm.23270.
Cohen, J., 1998. Statistical Power Analysis for the Behavioral Sciences, 2nd ed.,. L. Erlbaum Associates,. ⟨http://www.utstat.toronto.edu/~brunner/oldclass/378f16/readings/CohenPower.pdf⟩.
Conradi, H.J., Ormel, J., de Jonge, P., 2011. Presence of individual (residual) symptoms during depressive episodes and periods of remission: a 3-year prospective study. Psychol. Med. 41 (6), 1165–1174. https://doi.org/10.1017/S0033291710001911.
De Bartolo, P., Mandolesi, L., Federico, F., Foti, F., Cutuli, D., Gelfo, F., Petrosini, L., 2009. Cerebellar involvement in cognitive flexibility. Neurobiol. Learn. Mem. 92 (3), 310–317. https://doi.org/10.1016/j.nlm.2009.03.008.
Dennehy, E.B., Robinson, R.L., Stephenson, J.J., Faries, D., Grabner, M., Palli, S.R., Stauffer, V.L., Marangell, L.B., 2015. Impact of non-remission of depression on costs and resource utilization: from the comorbidities and symptoms of depression (CODE) study. Curr. Med. Res. Opin. 31 (6), 1165–1177. https://doi.org/10.1185/03007995.2015.1029893.
Diagnostic and statistical manual of mental disorders, 2000(4th ed.). (2000).
Fava, M., Graves, L.M., Benazzi, F., Scalia, M.J., Iosifescu, D.V., Alpert, J.E., Papakostas, G.I., 2006. A cross-sectional study of the prevalence of cognitive and physical symptoms during long-term antidepressant treatment. J. Clin. Psychiatry 67 (11), 0-0.
Gautam, S., Jain, A., Gautam, M., Vahia, V.N., Grover, S., 2017. Clinical practice guidelines for the management of depression. Indian J. Psychiatry 59 (Suppl 1), S34–S50. https://doi.org/10.4103/0019-5545.196973.
Godlewska, B.R., Browning, M., Norbury, R., Cowen, P.J., Harmer, C.J., 2016. Early changes in emotional processing as a marker of clinical response to SSRI treatment in depression. Transl. Psychiatry 6 (11), e957. https://doi.org/10.1038/tp.2016.130.
Griffanti, L. (2019, July 9). MELODIC - FslWiki. ⟨https://fsl.fmrib.ox.ac.uk/fsl/fslwiki/MELODIC⟩.
Gualtieri, C.T., Johnson, L.G., 2006. Reliability and validity of a computerized neurocognitive test battery, CNS vital signs. Arch. Clin. Neuropsychol.: Off. J. Natl. Acad. Neuropsychol. 21 (7), 623–643. https://doi.org/10.1016/j.acn.2006.05.007.
Gudayol-Ferré, E., Guàrdia-Olmos, J., Peró-Cebollero, M., 2015. Effects of remission speed and improvement of cognitive functions of depressed patients. Psychiatry Res. 226 (1), 103–112. https://doi.org/10.1016/j.psychres.2014.11.079.
Hair, J., Black, W., Babin, B., Anderson, R., 2009. Multivariate Data Analysis, 7th ed..,. Pearson,. ⟨https://www.pearson.ch/HigherEducation/Pearson/EAN/9780138132637/Multivariate-Data-Analysis⟩.
Hasselbalch, B.J., Knorr, U., Kessing, L.V., 2011. Cognitive impairment in the remitted state of unipolar depressive disorder: a systematic review. J. Affect. Disord. 134 (1–3), 20–31. https://doi.org/10.1016/j.jad.2010.11.011.
Honey, C.J., Sporns, O., Cammoun, L., Gigandet, X., Thiran, J.P., Meuli, R., Hagmann, P., 2009. Predicting human resting-state functional connectivity from structural connectivity. Proc. Natl. Acad. Sci. USA 106 (6), 2035–2040. https://doi.org/10.1073/pnas.0811168106.
Ito, M., 2002. Hopes for cerebellar research in the 21st century. Cerebellum (Lond., Engl.) 1 (2), 93–94. https://doi.org/10.1080/147342202753671213.
Iverson, G.L., Brooks, B.L., Young, A.H., 2009. Identifying neurocognitive impairment in depression using computerized testing. Appl. Neuropsychol. 16 (4), 254–261. https://doi.org/10.1080/09084280903297594.
Jackson, D.A., 1993. Stopping rules in principal components analysis: a comparison of heuristical and statistical approaches. Ecology 74 (8), 2204–2214. https://doi.org/10.2307/1939574.
Jaeger, J., Berns, S., Uzelac, S., Davis-Conway, S., 2006. Neurocognitive deficits and disability in major depressive disorder. Psychiatry Res. 145 (1), 39–48. https://doi.org/10.1016/j.psychres.2005.11.011.
James, S.L., Abate, D., Abate, K.H., Abay, S.M., Abbafati, C., Abbasi, N., Abbastabar, H., Abd-Allah, F., Abdela, J., Abdelalim, A., Abdollahpour, I., Abdulkader, R.S., Abebe, Z., Abera, S.F., Abil, O.Z., Abraha, H.N., Abu-Raddad, L.J., Abu-Rmeileh, N. M.E., Accrombessi, M.M.K., Murray, C.J.L., 2018. Global, regional, and national incidence, prevalence, and years lived with disability for 354 diseases and injuries for 195 countries and territories, 1990–2017: A systematic analysis for the Global Burden of Disease Study 2017. Lancet 392 (10159), 1789–1858. https://doi.org/10.1016/S0140-6736(18)32279-7.
Jenkinson, M., Bannister, P., Brady, M., Smith, S., 2002. Improved optimization for the robust and accurate linear registration and motion correction of brain images. NeuroImage 17 (2), 825–841. https://doi.org/10.1006/nimg.2002.1132.
Kaiser, R.H., Andrews-Hanna, J.R., Wager, T.D., Pizzagalli, D.A., 2015a. Large-scale network dysfunction in major depressive disorder: a meta-analysis of resting-state functional connectivity. JAMA Psychiatry 72 (6), 603–611. https://doi.org/10.1001/jamapsychiatry.2015.0071.
Kaiser, R.H., Andrews-Hanna, J.R., Wager, T.D., Pizzagalli, D.A., 2015b. Large-scale network dysfunction in major depressive disorder: meta-analysis of resting-state functional connectivity. JAMA Psychiatry 72 (6), 603–611. https://doi.org/10.1001/jamapsychiatry.2015.0071.
Kaplan, C., Zhang, Y., 2012. Assessing the comparative-effectiveness of antidepressants commonly prescribed for depression in the Us medicare population. J. Ment. Health Policy Econ. 15 (4), 171–178.
Karim, H.T., Andreescu, C., Tudorascu, D., Smagula, S.F., Butters, M.A., Karp, J.F., Reynolds, C., Aizenstein, H.J., 2017. Intrinsic functional connectivity in late-life depression: Trajectories over the course of pharmacotherapy in remitters and non-remitters. Mol. Psychiatry 22 (3), 450–457. https://doi.org/10.1038/mp.2016.55.
Kassambara, A., 2017. Practical Guide To Principal Component Methods in R: PCA, M (CA), FAMD, MFA, HCPC, factoextra. STHDA.
Kennedy, S.H., Lam, R.W., McIntyre, R.S., Tourjman, S.V., Bhat, V., Blier, P., Hasnain, M., Jollant, F., Levitt, A.J., MacQueen, G.M., McInerney, S.J., McIntosh, D., Milev, R.V., Müller, D.J., Parikh, S.V., Pearson, N.L., Ravindran, A.V., Uher, R., 2016. Canadian network for mood and anxiety treatments (CANMAT) 2016 clinical guidelines for the management of adults with major depressive disorder. Can. J. Psychiatry Rev. Can. De. Psychiatr. 61 (9), 540–560. https://doi.org/10.1177/0706743716659417.
Khoo, A.L., Zhou, H.J., Teng, M., Lin, L., Zhao, Y.J., Soh, L.B., Mok, Y.M., Lim, B.P., Gwee, K.P., 2015. Network meta-analysis and cost-effectiveness analysis of new generation antidepressants. CNS Drugs 29 (8), 695–712. https://doi.org/10.1007/s40263-015-0267-6.
Korgaonkar, M.S., Goldstein-Piekarski, A.N., Fornito, A., Williams, L.M., 2020. Intrinsic connectomes are a predictive biomarker of remission in major depressive disorder. Mol. Psychiatry 25 (7), 1537–1549. https://doi.org/10.1038/s41380-019-0574-2.
Korgaonkar, M.S., Williams, L.M., Song, Y.J., Usherwood, T., Grieve, S.M., 2014. Diffusion tensor imaging predictors of treatment outcomes in major depressive disorder. Br. J. Psychiatry 205 (4), 321–328. https://doi.org/10.1192/bjp.bp.113.140376.
Krause-Sorio, B., Siddarth, P., Milillo, M.M., Vlasova, R., Ercoli, L., Narr, K.L., Lavretsky, H., 2020. Regional white matter integrity predicts treatment response to escitalopram and memantine in geriatric depression: a pilot study. Front. Psychiatry 11, 548904. https://doi.org/10.3389/fpsyt.2020.548904.
Kubitz, N., Mehra, M., Potluri, R.C., Garg, N., Cossrow, N., 2013. Characterization of treatment resistant depression episodes in a cohort of patients from a us commercial claims database. PLOS ONE 8 (10), e76882. https://doi.org/10.1371/journal.pone.0076882.
Lam, R., Milev, R., Rotzinger, S., Andreazza, A., Blier, P., Brenner, C., Daskalakis, Z., Dharsee, M., Downar, J., Evans, K., Farzan, F., Foster, J., Frey, B., Geraci, J., Giacobbe, P., Feilotter, H., Hall, G., Harkness, K., Hassel, S., Kennedy, S., 2016. Discovering biomarkers for antidepressant response: protocol from the Canadian biomarker integration network in depression (CAN-BIND) and clinical characteristics of the first patient cohort. BMC Psychiatry 16. https://doi.org/10.1186/s12888-016-0785-x.

Lee, R.S.C., Hermens, D.F., Porter, M.A., Redoblado-Hodge, M.A., 2012. A meta-analysis of cognitive deficits in first-episode major depressive disorder. J. Affect. Disord. 140 (2), 113–124. https://doi.org/10.1016/j.jad.2011.10.023.

Li, L., Su, Y.-A., Wu, Y.-K., Castellanos, F.X., Li, K., Li, J.-T., Si, T.-M., Yan, C.-G., 2021. Eight-week antidepressant treatment reduces functional connectivity in first-episode drug-naïve patients with major depressive disorder. Hum. Brain Mapp. 42 (8), 2593–2605. https://doi.org/10.1002/hbm.25391.

Lisiecka, D., Meisenzahl, E., Scheuerecker, J., Schoepf, V., Whitty, P., Chaney, A., Moeller, H.-J., Wiesmann, M., Frodl, T., 2011. Neural correlates of treatment outcome in major depression. Int. J. Neuropsychopharmacol. 14 (4), 521–534. https://doi.org/10.1017/S1461145710001513.

MacQueen, G.M., Hassel, S., Arnott, S.R., Addington, J., Bowie, C.R., Bray, S.L., Davis, A. D., Downar, J., Foster, J.A., Frey, B.N., Goldstein, B.I., Hall, G.B., Harkness, K.L., Harris, J., Lam, R.W., Lebel, C., Milev, R., Müller, D.J., Parikh, S.V., Kennedy, S., 2019. The Canadian Biomarker Integration Network in Depression (CAN-BIND): magnetic resonance imaging protocols. J. Psychiatry Neurosci.: JPN 44 (4), 223–236. https://doi.org/10.1503/jpn.180036.

Marek, S., Tervo-Clemmens, B., Calabro, F.J., Montez, D.F., Kay, B.P., Hatoum, A.S., Donohue, M.R., Foran, W., Miller, R.L., Hendrickson, T.J., Malone, S.M., Kandala, S., Feczko, E., Miranda-Dominguez, O., Graham, A.M., Earl, E.A., Perrone, A.J., Cordova, M., Doyle, O., Dosenbach, N.U.F., 2022. Reproducible brain-wide association studies require thousands of individuals. Nature 603 (7902), 654–660. https://doi.org/10.1038/s41586-022-04492-9.

Mauskopf, J.A., Simon, G.E., Kalsekar, A., Nimsch, C., Dunayevich, E., Cameron, A., 2009. Nonresponse, partial response, and failure to achieve remission: Humanistic and cost burden in major depressive disorder. Depress Anxiety 26 (1), 83–97. https://doi.org/10.1002/da.20505.

McCall, W.V., Dunn, A.G., 2003. Cognitive deficits are associated with functional impairment in severely depressed patients. Psychiatry Res. 121 (2), 179–184. https://doi.org/10.1016/j.psychres.2003.09.003.

McIntyre, R.S., Cha, D.S., Soczynska, J.K., Woldeyohannes, H.O., Gallaugher, L.A., Kudlow, P., Alsuwaidan, M., Baskaran, A., 2013. Cognitive deficits and functional outcomes in major depressive disorder: determinants, substrates, and treatment interventions: review: cognitive deficits and functional outcomes in MDD. Depress Anxiety 30 (6), 515–527. https://doi.org/10.1002/da.22063.

McIntyre, R.S., Fallu, A., Konarski, J.Z., 2006. Measurable outcomes in psychiatric disorders: remission as a marker of wellness. Clin. Ther. 28 (11), 1882–1891. https://doi.org/10.1016/j.clinthera.2006.11.007.

Menon, V., Uddin, L.Q., 2010. Saliency, switching, attention and control: a network model of insula function. Brain Struct. Funct. 214, 655–667.

Middleton, H., Shaw, I., Hull, S., Feder, G., 2005. NICE guidelines for the management of depression. BMJ: Br. Med. J. 330 (7486), 267–268.

Montgomery, S.A., Asberg, M., 1979. A new depression scale designed to be sensitive to change. Br. J. Psychiatry.: J. Ment. Sci. 134, 382–389. https://doi.org/10.1192/bjp.134.4.382.

Naismith, S.L., Longley, W.A., Scott, E.M., Hickie, I.B., 2007. Disability in major depression related to self-rated and objectively-measured cognitive deficits: A preliminary study. BMC Psychiatry 7, 32. https://doi.org/10.1186/1471-244X-7-32.

Ombao, H., Lindquist, M., Thompson, W., Aston, J., 2016. Handbook of Neuroimaging Data Analysis. CRC Press.

Persson, J., Struckmann, W., Gingnell, M., Fällmar, D., Bodén, R., 2020. Intermittent theta burst stimulation over the dorsomedial prefrontal cortex modulates resting-state connectivity in depressive patients: a sham-controlled study. Behav. Brain Res. 394, 112834 https://doi.org/10.1016/j.bbr.2020.112834.

R Core Team. (2018). *R: A Language and Environment for Statistical Computing.* ⟨https://www.r-project.org/⟩.

Ray, K., McKay, D., Fox, P., Riedel, M., Uecker, A., Beckmann, C., Smith, S., Fox, P., Laird, A., 2013. ICA model order selection of task co-activation networks. Front. Neurosci. 7. ⟨https://www.frontiersin.org/articles/10.3389/fnins.2013.00237⟩.

Refaat, M., 2010. Data Preparation for Data Mining Using SAS. Elsevier,.

Reppermund, S., Ising, M., Lucae, S., Zihl, J., 2009. Cognitive impairment in unipolar depression is persistent and non-specific: further evidence for the final common pathway disorder hypothesis. Psychol. Med. 39 (4), 603–614. https://doi.org/10.1017/S003329170800411X.

Robbins, T.W., Gillan, C.M., Smith, D.G., de Wit, S., Ersche, K.D., 2012. Neurocognitive endophenotypes of impulsivity and compulsivity: towards dimensional psychiatry. Trends Cogn. Sci. 16 (1), 81–91. https://doi.org/10.1016/j.tics.2011.11.009.

Rush, A.J., Trivedi, M.H., Wisniewski, S.R., Nierenberg, A.A., Stewart, J.W., Warden, D., Niederehe, G., Thase, M.E., Lavori, P.W., Lebowitz, B.D., McGrath, P.J., Rosenbaum, J.F., Sackeim, H.A., Kupfer, D.J., Luther, J., Fava, M., 2006. Acute and longer-term outcomes in depressed outpatients requiring one or several treatment steps: A STAR*D Report. Am. J. Psychiatry 163 (11), 1905–1917. https://doi.org/10.1176/ajp.2006.163.11.1905.

Schloerke, B., Cook, D., Larmarange, J., Briatte, F., Marbach, M., Thoen, E., Elberg, A., Toomet, O., Crowley, J., Hofmann, H., & Wickham, H. (2018). *GGally: Extension to "ggplot2."* ⟨https://CrAn.r-project.org/package=GGally⟩.

Schmahmann, J.D., 2004. Disorders of the cerebellum: Ataxia, dysmetria of thought, and the cerebellar cognitive affective syndrome. J. Neuropsychiatry Clin. Neurosci. 16 (3), 367–378. https://doi.org/10.1176/jnp.16.3.367.

Sheehan, D.V., Lecrubier, Y., Sheehan, K.H., Amorim, P., Janavs, J., Weiller, E., Hergueta, T., Baker, R., Dunbar, G.C., 1998. The mini-international neuropsychiatric interview (M.I.N.I.): the development and validation of a structured diagnostic psychiatric interview for DSM-IV and ICD-10. J. Clin. Psychiatry 59 Suppl 20, 22–33 quiz 34-57.

Smith, S.M., Fox, P.T., Miller, K.L., Glahn, D.C., Fox, P.M., Mackay, C.E., Filippini, N., Watkins, K.E., Toro, R., Laird, A.R., Beckmann, C.F., 2009. Correspondence of the brain's functional architecture during activation and rest. Proc. Natl. Acad. Sci. 106 (31), 13040–13045. https://doi.org/10.1073/pnas.0905267106.

Snyder, H.R., 2013. Major depressive disorder is associated with broad impairments on neuropsychological measures of executive function: A meta-analysis and review. Psychol. Bull. 139 (1), 81–132. https://doi.org/10.1037/a0028727.

Stahl, S.M., 1999. Why Settle for silver, when you can go for gold? response vs. recovery as the goal of antidepressant therapy: (Brainstorms). J. Clin. Psychiatry 60 (4), 213–214. https://doi.org/10.4088/JCP.v60n0401.

Strother, S.C., 2006. Evaluating fMRI preprocessing pipelines. IEEE Eng. Med. Biol. Mag.: Q. Mag. Eng. Med. Biol. Soc. 25 (2), 27–41. https://doi.org/10.1109/memb.2006.1607667.

Taylor, P.A., Saad, Z.S., 2013. FATCAT: (an efficient) functional and tractographic connectivity analysis toolbox. Brain Connect. 3 (5), 523–535. https://doi.org/10.1089/brain.2013.0154.

Teipel, S.J., Bokde, A.L.W., Meindl, T., Amaro, E., Soldner, J., Reiser, M.F., Herpertz, S. C., Möller, H.-J., Hampel, H., 2010. White matter microstructure underlying default mode network connectivity in the human brain. NeuroImage 49 (3), 2021–2032. https://doi.org/10.1016/j.neuroimage.2009.10.067.

Thach, W.T., 2007. On the mechanism of cerebellar contributions to cognition. Cerebellum 6 (3), 163–167. https://doi.org/10.1080/14734220701373530.

Thase, M.E., Haight, B.R., Richard, N., Rockett, C.B., Mitton, M., Modell, J.G., VanMeter, S., Harriett, A.E., Wang, Y., 2005. Remission rates following antidepressant therapy with bupropion or selective serotonin reuptake inhibitors: a meta-analysis of original data from 7 randomized controlled trials. J. Clin. Psychiatry 66 (8), 0-0.

Thase, M.E., Nierenberg, A.A., Vrijland, P., van Oers, H.J.J., Schutte, A.-J., Simmons, J. H., 2010. Remission with mirtazapine and selective serotonin reuptake inhibitors: a meta-analysis of individual patient data from 15 controlled trials of acute phase treatment of major depression. Int. Clin. Psychopharmacol. 25 (4), 189–198. https://doi.org/10.1097/YIC.0b013e328330adb2.

Trivedi, M.H., Rush, A.J., Wisniewski, S.R., Nierenberg, A.A., Warden, D., Ritz, L., Norquist, G., Howland, R.H., Lebowitz, B., McGrath, P.J., Shores-Wilson, K., Biggs, M.M., Balasubramani, G.K., Fava, M., Study Team, S.T.A.R.*D., 2006. Evaluation of outcomes with citalopram for depression using measurement-based care in STAR*D: implications for clinical practice. Am. J. Psychiatry 163 (1), 28–40. https://doi.org/10.1176/appi.ajp.163.1.28.

Wang, L., Li, K., Zhang, Q., Zeng, Y., Dai, W., Su, Y., Wang, G., Tan, Y., Jin, Z., Yu, X., Si, T., 2014. Short-term effects of escitalopram on regional brain function in first-episode drug-naive patients with major depressive disorder assessed by resting-state functional magnetic resonance imaging. Psychol. Med. 44 (7), 1417–1426. https://doi.org/10.1017/S0033291713002031.

Wang, L., Xia, M., Li, K., Zeng, Y., Su, Y., Dai, W., Zhang, Q., Jin, Z., Mitchell, P.B., Yu, X., He, Y., Si, T., 2014. The effects of antidepressant treatment on resting-state functional brain networks in patients with major depressive disorder. Hum. Brain Mapp. 36 (2), 768–778. https://doi.org/10.1002/hbm.22663.

Webster, M. (2012, August 13). *FMRIB58_FA - FslWiki.* ⟨https://fsl.fmrib.ox.ac.uk/fsl/fslwiki/FMRIB58_FA⟩.

Xiao, X., Bentzley, B.S., Cole, E.J., Tischler, C., Stimpson, K.H., Duvio, D., Bishop, J.H., DeSouza, D.D., Schatzberg, A., Keller, C., Sudheimer, K.D., Williams, N.R., 2019. Functional connectivity changes with rapid remission from moderate-to-severe major depressive disorder [Preprint]. Clin. Trials. https://doi.org/10.1101/672154.

Yeo, B.T.T., Krienen, F.M., Sepulcre, J., Sabuncu, M.R., Lashkari, D., Hollinshead, M., Roffman, J.L., Smoller, J.W., Zöllei, L., Polimeni, J.R., Fischl, B., Liu, H., Buckner, R. L., 2011. The organization of the human cerebral cortex estimated by intrinsic functional connectivity. J. Neurophysiol. 106 (3), 1125–1165. https://doi.org/10.1152/jn.00338.2011.

Zheng, K., Wang, H., Liu, J., Xi, Y., Li, L., Zhang, X., Li, J., Yin, H., Tan, Q., Lu, H., Li, B., 2018. Incapacity to control emotion in major depression may arise from disrupted white matter integrity and OFC-amygdala inhibition. CNS Neurosci. Ther. 24 (11), 1053–1062. https://doi.org/10.1111/cns.12800.

Zimmerman, M., McGlinchey, J.B., Posternak, M.A., Friedman, M., Attiullah, N., Boerescu, D., 2006. How should remission from depression be defined? the depressed patient's perspective. Am. J. Psychiatry 163 (1), 148–150. https://doi.org/10.1176/appi.ajp.163.1.148.